

# Behaviour of a Moveable Barrier on Revetment for Mitigation of Disaster by Wave Overtopping

J.H. Seo<sup>1</sup>, D.H. Won<sup>1</sup> and W.S. Park<sup>1</sup>

<sup>1</sup> KIOST (Korea Institute of Ocean Science and Technology), Yeongdo, Busan, Republic of Korea

## Abstract

Recently, port city has been gradually expanding near coastal area, and many facilities for the purpose of tour and waterfront have been constructed near the shore. When the storm surge developed by typhoon have occurred, coastal facilities have a lot of damage and failure with loss of life caused directly by the waves. Various barrier design concepts have been suggested to protect property and human life from disasters, they have not been widely applied though. Because they do not satisfy the recent trends that emphasize the surrounding scenery. In this study, a moveable barrier on revetment is proposed against wave overtopping. This moveable barrier has two main functions, sightseeing and protecting. In case of usual day, it is installed on the revetment and used observatory deck for sightseeing. When wave overtopping has occurred by storm surge, it protect coastal area through changing of flat deck to triangular barrier. The hydraulic and the structural performance of the newly proposed movable barrier was investigated through numerical analysis using commercial program. As a results, this structure has good performance. However, it is at a conceptual level, and there are still uncertainties related to aspects such as feasibility and engineering performance.

## 1 Instruction

A port city which consists of a port and the hinterland, has been developed through interaction from the past. According to the development stage of the port city, although the port and the city were located in the same space at the initial stage. Due to the rapid expansion of the port, they had separated the city and port space (Hoyle, 1989). Since the 1980s, as the port has lost its port function due to the enlargement and de-industrialization of ships, the port has begun to be actively develop into the space with a waterfront function. With this tendency, the port city is gradually expanding around the coastal area and many tourist facilities and residential facilities are being built near the waterfront. This may lead to be directly damaged to the revetment structures and buildings in case of typhoons or storms. Typhoons hit the Korean Peninsula every year by geographic location. In particular, the 18th Typhoon CHABA which hit on the Korea Peninsular in 2016 was caused flood damage by the wave overtopping and has wreaked havoc on the facilities lo-

cated near the shore. When it comes to engineering design, higher barriers must be installed in this area. However, this is the case that the barriers are lower than the design height due to tourism and residents' demands, causing damage by the wave overtopping. In this way, it can be considered that a new type of disaster prevention structure might be needed in areas where high barriers cannot be installed by the urban development and demand with sea views. In this study, a movable barrier which is an onshore structure and can be used as a sightseeing type deck at ordinary times, was proposed and analyzed that can stand up and stop to prevent wave overtopping during abnormal times.

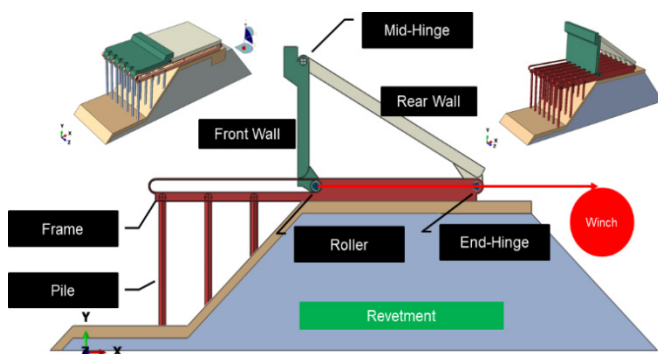
## 2 Hydraulic performance analysis

### 2.1 Outline of a movable barrier on revetment

A movable barrier system on revetment proposed in this study can be described in terms of before and after operation for movement of the structure. At first, the before operation of the movable barrier means an ordinary state in which any wave overtopping is applied on

revetment as shown in upper left corner of **Figure 1**. It can be installed as a form of sightseeing deck and can be used for public recreational purposes such as jogging and walking along the deck. On the other hand, at the time of the occurrence of wave overtopping or the forecasting, the operation work for standing up starts and that means an abnormal state. When the cable connected to the winch which is located at the back of the barrier is rolled, the front wall of the barrier will move and work until the angle of the front wall becomes about 85 degrees. In this case, the barrier system has the upper and lower guide rails to maintain the shape of the system according to the movement of roller, and has formed the grid-shaped frame as a whole by being fixed to the pier for the seaside part and on the revetment for the landside part. Then, when the abnormal state that may cause the wave overtopping is terminated, rotation of the winch reduces the cable tension so that the movable barrier system slowly returns to its original shape due to its own weight. Here, the pier pile and the frame are a structure made by steel, and the front and rear walls are a composite of steel and concrete structure.

Figure 1. Constitution of the moveable barrier system on revetment



## 2.2 Calculation of pressure on the front wall by numerical experiment

In this study, CADMAS-SURF (Coastal Development Institute of Technology, 2001) was used to rationally derive the pressure on the front wall by wave when a storm occurred. This commercial program has a numerical model based on the Navier-Stokes equations for two-dimensional incompressible viscous flow, which increases the shape approximation of structures based on the Porous model (Sha et al., 1978, Sakakiyama et al., 1990). VOF (Volume of Fluid) method

is used to analyze complex free surface (Hirt and Nichols, 1981), and the reflection wave from the structure was controlled the problem of re-reflection at the wave boundary using the Sommerfeld radiation boundary and the energy attenuation band. And Dupuit-Forchheimer type resistance rule was added in CADMAS-SURF ver. 5.1 (Coastal Development Institute of Technology, 2001). Unlike the conventional drag force equation, the equation proposed by Engelund (1953), was applied, which expresses the relationship between the size of the constituent material of the transmission structure and the resistance coefficient.

Figure 2 illustrates a target revetment of a random port on the West coastal in Korea. The water depth of the target area can be calculated by referring to the regional design tidal data of the Aramir project (MLTM, 2011). As shown in Figure 3, storm surge height and sea level rise were applied, and the water depth at this time was 8.067 m. In this numerical simulation, the regular and irregular waves are considered and the experimental area is shown in Figure 4. The portion marked with black in Figure 2 means the pier part on the revetment and is treated as an impermeable structure for convenience of calculation.

Figure 2. Cross section properties (revetment)

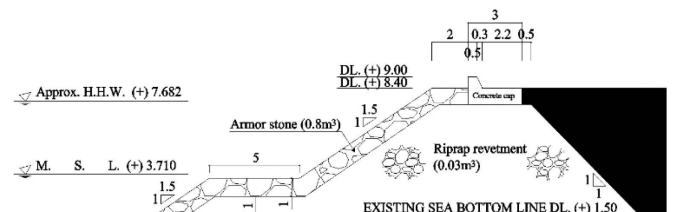
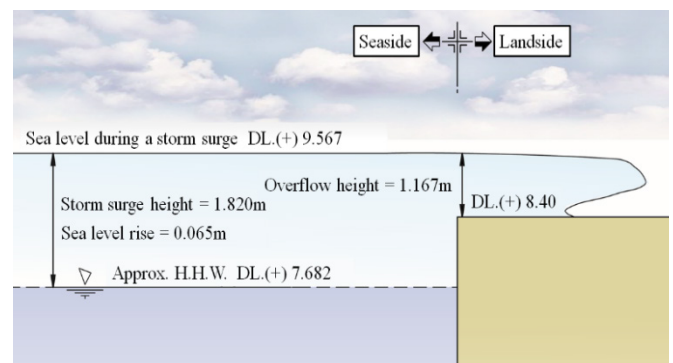


Figure 3. Sea level properties during a storm surge



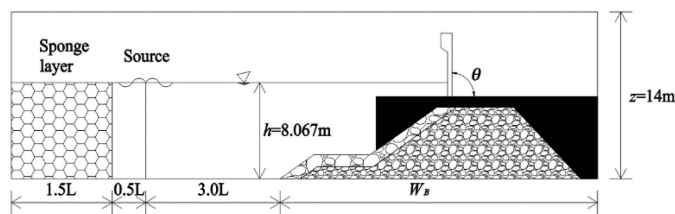
In regular wave experiment, the incident wave was generated at the left boundary due to internal wave

generation with nonlinearity. Also, the irregular wave experiment performed internal wave generation and left the energy attenuation band on the left side. The design wave with 50 years return period was applied, the design wave height and wave period is 2.0 m and 6.73 sec respectively. The structure of the part excluding the crushed rock was simplified as an impermeable structure. The width of the revetment ( $W_B$ ) was set to 28.4 m. The particle size of armor stones and riprap for the revetment were each 0.93 m and 0.31 m. And the porosity was assumed to be 0.37 equally. Numerical experiments were carried out in four cases according to the slope angle of movable barriers as  $\theta = 60^\circ, 70^\circ, 80^\circ, 90^\circ$ . The details of the numerical experiment are shown in [Table 1](#).

Table 1. Dimensions for numerical experiments.

Regular wave	Stream 22
Irregular wave	Bretschneider-Mitsuyasu
Significant wave height (m)	2.0
Significant wave period (s)	6.73
Density of fluid (kg/m <sup>3</sup> )	1027.0
Turbulent model	$k - \epsilon$
Inertia coefficient, $C_M$	1.2
Drag coefficient, $\alpha_0, \beta_0$	1500, 3.6
Porosity	0.37
Kinematic viscosity (m <sup>2</sup> /s)	1.3604E-06

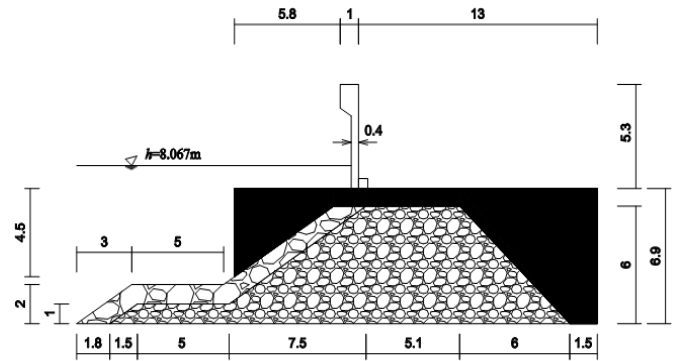
Figure 4. Computational domain



The grid size was constructed at equal intervals as  $\Delta x = 0.2$  m,  $\Delta z = 0.1$  m to represent the slope of the movable barrier. The analysis times of the regular wave and the irregular wave are respectively 100 sec and 130 sec, the regular wave experiment analyzed the results until the reflective wave reaches the structure. And the number of component waves of irregular

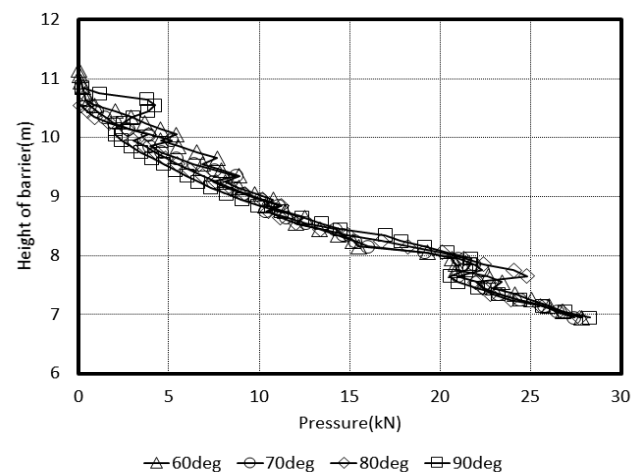
waves is 200. The detailed dimensions according to the slope of the movable barrier are shown in [Figure 5](#).

Figure 5. Detailed dimensions for test cases



To analyze the structural behavior of the proposed movable barrier, it is necessary to investigate the magnitude of the pressure acting on the front wall of the barriers. The pressure was measured in all elements located at the front wall of the barriers and the results were derived using the data after the numerical solution was stable. Since the hydrostatic pressure by the water level rise directly affects the movable barrier system, the hydrostatic pressure was included in this pressure. [Figure 6](#) illustrates the average maximum pressure at the front wall of the barrier in the regular wave experiment, and [Figure 7](#) expresses the maximum pressure at the front wall of the barrier in an irregular wave experiment. Since the barrier was installed from the bottom of revetment ( $z = 6.9$  m), [Figure 6](#) and [Figure 7](#) show that the pressure has the highest pressure at the lowest point.

Figure 6. Average maximum pressure for the regular wave



The maximum pressure distributions acting on the

regular and irregular waves are 27 kPa and 30 kPa, respectively, it can be seen that the case for irregular wave is larger than the case for regular wave.

Figure 7. Maximum pressure for the irregular wave

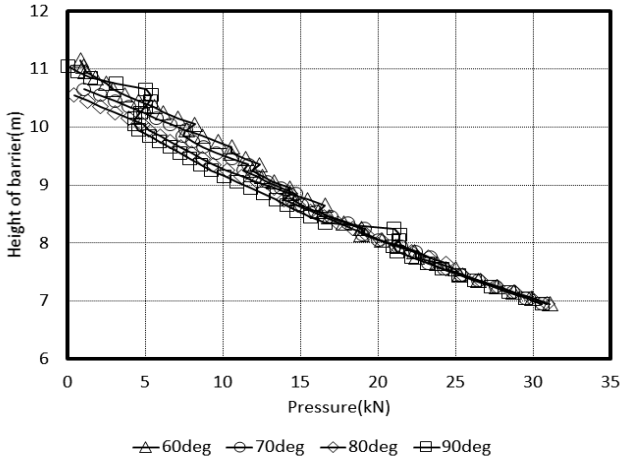


Figure 8. Time series pressure at lowest point of moveable barrier (regular wave)

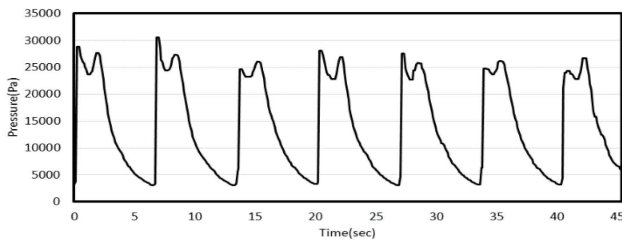
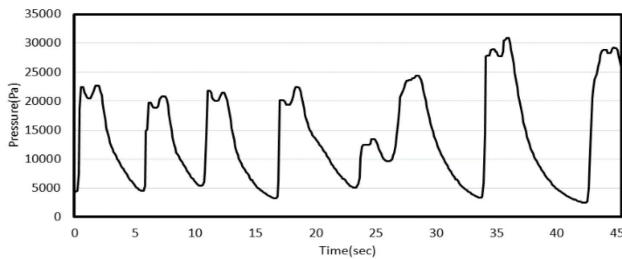


Figure 9. Time series pressure at lowest point of moveable barrier (irregular wave)



Also, there is a slight pressure difference depending on the slope of the barrier though, it can be found that the pressure distribution was almost similar regardless of the slope angle of the barrier. In this study, as shown in **Figure 8** and **Figure 9**, the structural behavior is analyzed by using the time-dependent pressure distribution as input data when the slope angle of the moveable barrier is 80 degrees.

### 3 Structural behaviour analysis

#### 3.1 Outline of structural analysis

To analyze the structural behaviour of movable barriers, a commercial finite element analysis program ABAQUS (Simulia, 2013) was used and simplified the modeling as shown in **Figure 10** excluding the revetment and pier pile parts in **Figure 1**. Thus, the analytical model consists of two roller frames, a front wall and a rear wall of the barrier. In this study, Structural behaviors of the barriers was analyzed divided into two parts. One is during standing-up operation before wave- overtopping, and another is after operation with wave overtopping for movement of the structure.

Figure 10. Boundary condition of analysis model

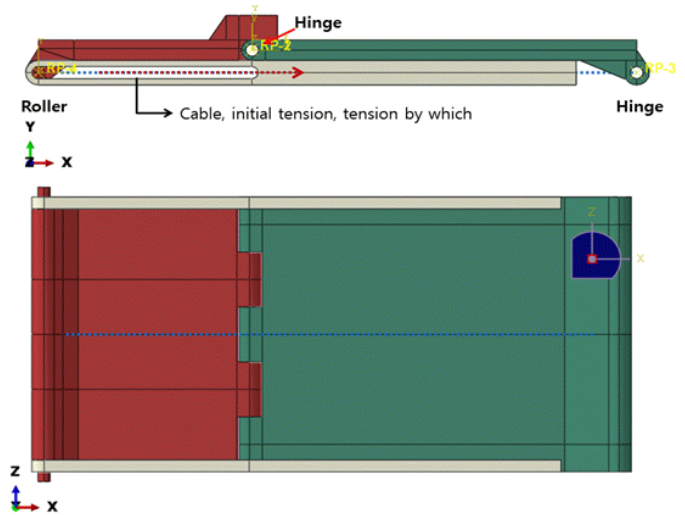


Table 2. Material properties for analysis.

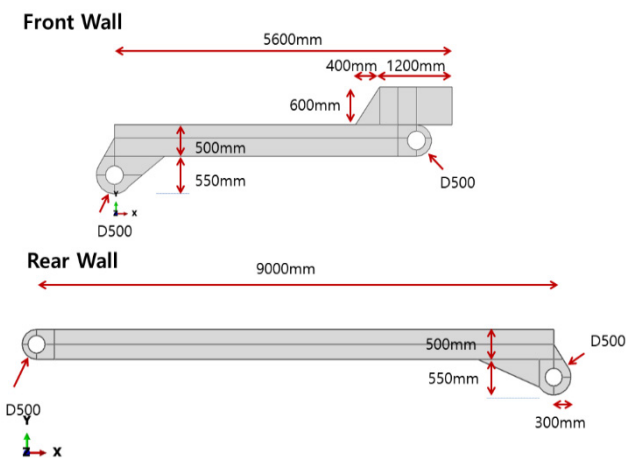
Material type	Properties
Mass density of steel (kg/m <sup>3</sup> )	7850
Elastic modulus of steel (GPa)	210
Poisson ratio of steel	0.3
Yield strength of steel (MPa)	320
Tensile strength of steel (MPa)	490
Mass density of concrete (kg/m <sup>3</sup> )	2400
Elastic modulus of concrete (MPa)	27536
Poisson ratio of concrete	0.17
Compressive strength of concrete (MPa)	30

The boundary condition of the analytical model (**Figure 10**) was composed two hinges and a roller. The roller

frame was assumed to be in a fixed state (6 direction), and the end hinge which is fixed on the revetment was constrained except for the rotation in the Z direction. The front and rear barriers are assumed to be rotatable using the connector option. The materials of the roller frame was supposed to be made steel frame, front and rear walls are assumed to be steel-concrete composite structures which was modeled as a form of an empty box at the top and be filled with concrete in an empty space. The detailed material properties for analysis are summarized in [Table 2](#).

The dimension of analytical model is illustrated in [Figure 11](#). The length of the front wall and rear wall are each 5.6 m and 9.0 m, and the thickness is same as 0.5 m. And the position of the mid hinge, end hinge and roller was adjusted to make it rise with a small force, which the middle hinge was modeled by installing about 600 mm above end hinge and roller. All models used 3D elements (C3D8R). It was analysed as a displacement load condition in which the barrier was pulled up by the cable in the [Figure 10](#) which was pulled 5 m for 10 minutes (600 seconds). After standing-up, the load of [Figure 9](#) i.e. irregular wave was applied to the entire barrier system for 100 seconds. This irregular wave pressure is the maximum pressure at the bottom ( $z = 6.9$  m). However, in this structural analysis, it is assumed that pressure acts evenly on the whole surface in terms of conservative aspects.

Figure 11. Dimension of analysis model

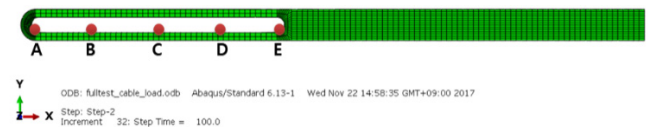


### 3.2 Behaviour analysis during standing-up operation

To determine the structural stability during standing-up operation, the stress condition occurring in the roller frame and the front and rear walls is most important

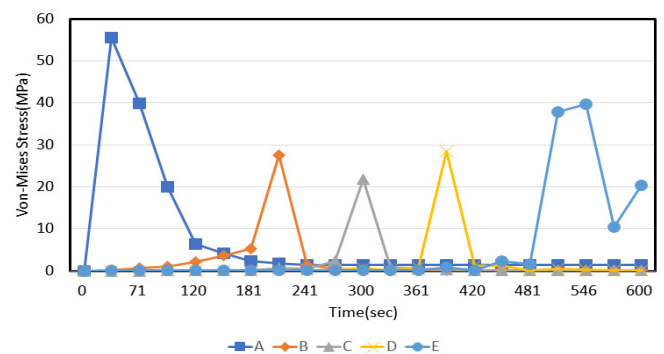
part. If the operation of barrier system cannot be performed efficiently, there is a great possibility that large stress was generated in the roller frame and the front and rear barrier walls. Therefore, the stress occurring in these two parts was analyzed in this study. At first, five points (A, B, C, D, E) for stress confirmation were selected as shown in [Figure 12](#) and was checked the Von-Mises stress acting on the roller frame during operation.

Figure 12. Investigation point on roller frame



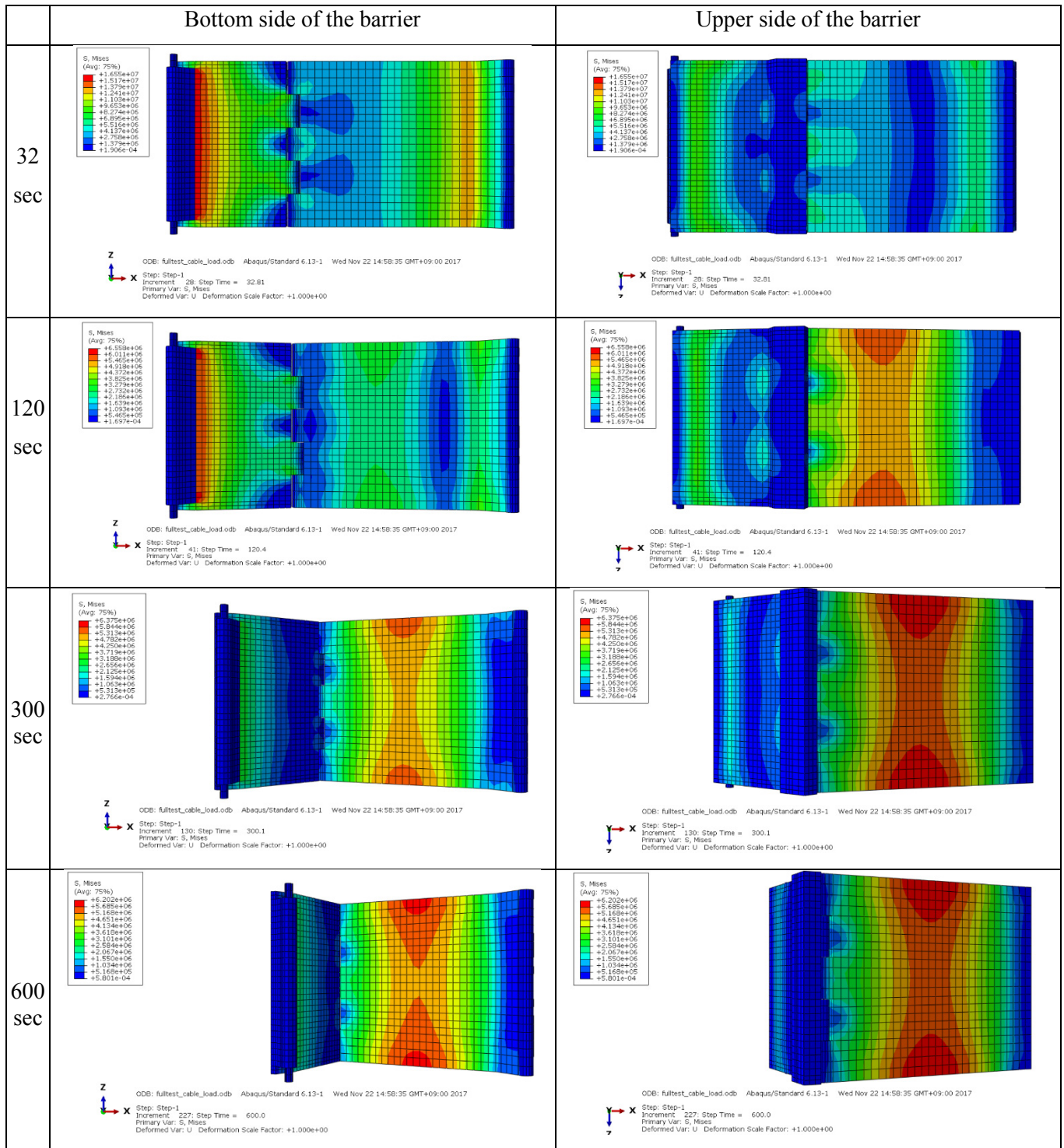
[Figure 13](#) shows the Von-Mises stress acting on the roller frame during operation. It can be found that at the start for the standing-up (when passing point A) and at the end of operation (when passing point E) have greatest stress. At each point, the stress increases as the barrier passes through the roller frame, passing through point A, where the first movement begins, and the stresses at point B, C, and D are reduced by 50% of the point A. The maximum stress at the point A and E quantitatively was generated 55 MPa and 40 MPa respectively. It can be judged to be safe that is equivalent to 17% of the yield strength of the steel, 320MPa. Therefore, it is considered that sufficient structural performance can be secured by simply changing the steel grade of the roller frame or reducing the cross-sectional area thereof.

Figure 13. Von-Mises stress at each point on roller frame



Next, the stress acting on the front and rear walls was analyzed in [Table 3](#) which shows the qualitative analysis of the maximum stress location.

Table 3. Distribution of Von-mises stress during standing-up operation



When the barrier system starts the standing-up operation, the roller of the front wall has generated the large stress by compressive force, and the rear wall part has generated the large stress after moving. To quantitatively analyse this, as shown Figure 14, a total of 8 stress check points were set from B-1 to B-4 on the bottom side of the barrier and from U-1 to U-4 on the upper side of the barrier.

As a result of the stress analysis, it can be found that the stress was generated small less than 16 MPa, and the check point B-1 and B-2, which are the boundary between the mid-hinge and the front and rear wall, are the most vulnerable. It is necessary to be considered in designing this part. In the case of the upper side of the barrier, the stress has increased with the standing-up operation, the magnitude of the stress was also small

under 6 MPa though. This stress distribution can be easily grasped in Table 3.

Figure 14 stress check point (up: bottom, down: upper)

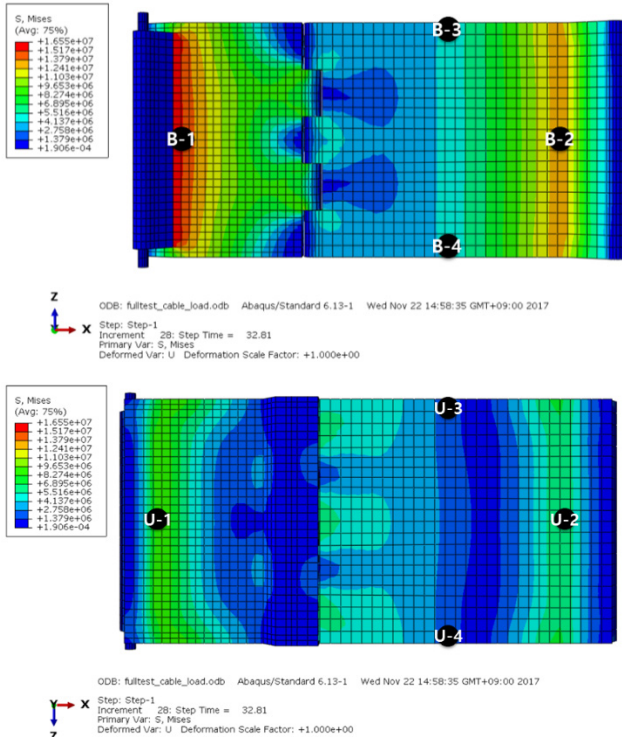


Figure 15 Von-Mises stress at each point during standing-up

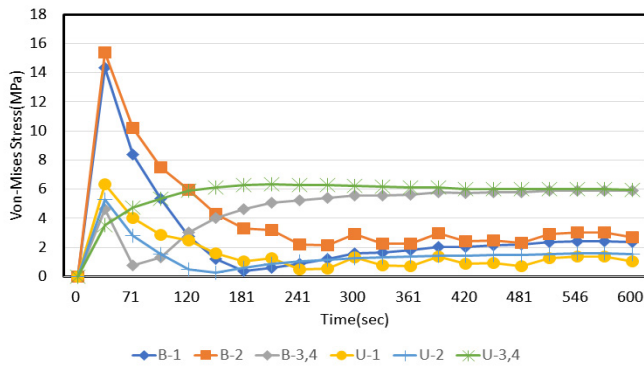
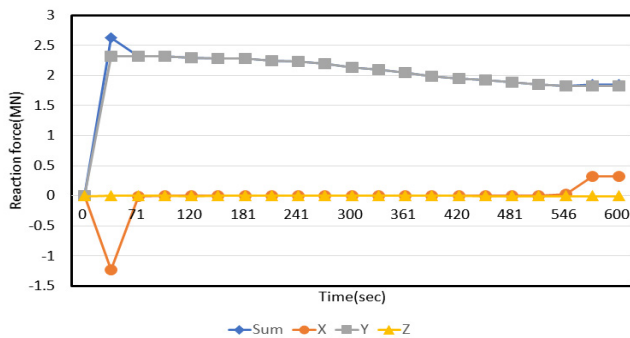


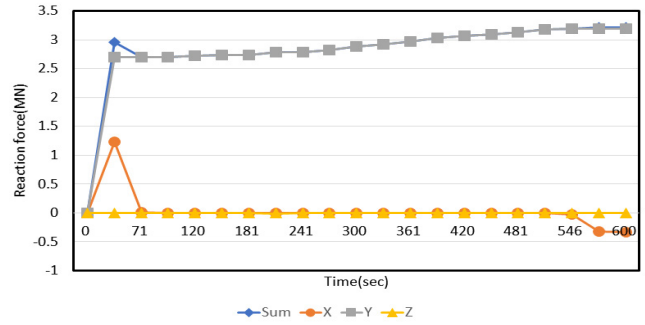
Figure 16 Reaction force at the end hinge



In the beginning of the standing-up operation, stress was concentrated at the joint part between the hinge

and the walls of the barrier, and then was decreased as the standing progressed. In the upper side of the barrier, the stress was mainly generated at the rear wall. The reason why the stress is generated in the early stage is as shown in Figure 16 the barrier system is under compressive force initially. It can be confirmed that the reaction force in the x direction becomes zero after the system starts to move.

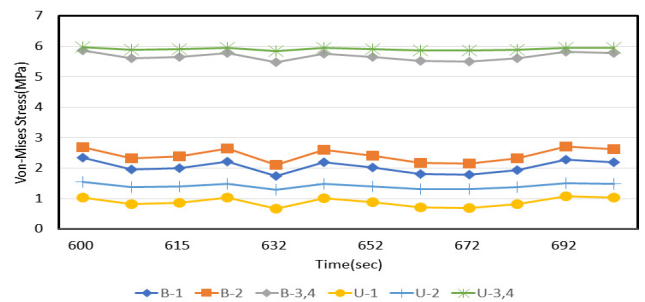
Figure 17 Reaction force at roller frame



### 3.3 Behaviour analysis after operation with wave overtopping

After the completion of the standing-up operation of the barrier in the above section, the irregular wave of Figure 9 has evenly applied to the front wall. Figure 18 displays the Von-Mises stress at each point under irregular wave, and it can be confirmed that the stress does not increase in the hinge or roller after standing-up.

Figure 18 Von-Mises stress at each point under irregular wave



Compared with Figure 15, it can be seen that the stress is maintained constantly. It can be judged that the continuous wave acting does not greatly affect the stress change of the barrier system. This little change in the stress acting on the barrier considered that because the continuous tension of the cable acts on the barrier. This can be checked by comparing Figure 17 with Figure 20.

Figure 19 Reaction force at the end hinge under irregular wave

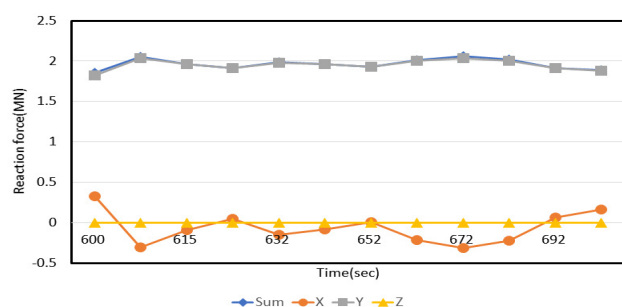
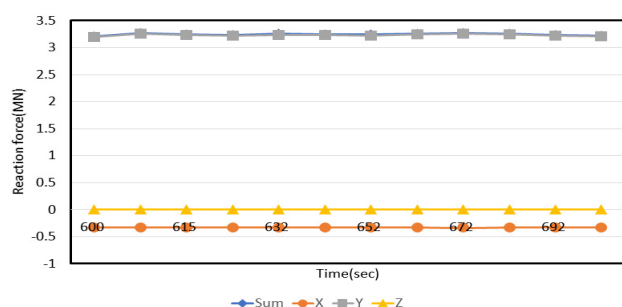


Figure 20 Reaction force at the roller frame under irregular wave



Since the tensile force of the cable is continuously applied to the system even after the standing-up operation, the reaction force in the x-direction is continuously acting on the roller frame. As a result of this condition, it can be seen that the reaction force in the x-direction is continuously fluctuated by the external wave loads as shown in Figure 19.

In this analysis, the stress and reaction force of the barrier model were analyzed during the standing-up operation and the after wave-overtopping operation. As a result, the greatest stress has occurred at the initial stage, but the model can be considered to be safe because the stress is small. In addition, the movable barrier of this triangular structure have been shown to cope with the wave overtopping appropriately, but the point reaction force generated at this time should be efficiently designed for the safety. Since the roller frame and the end hinge of the movable barrier system is resistant to most reaction forces, it is necessary to design a support structure that can securely fix them.

#### 4 Conclusion

In this study, behaviour of a moveable barrier structure on revetment for mitigation of disaster by wave overtopping was conducted using numerical analysis. Nu-

merical experiments were carried out to verify the hydraulic performance of the structure and to calculate the wave pressure acting on the front wall of the barrier. This pressure time series derived from these tests were applied to the completed standing-up barrier to analyse the structural performance. The stress distribution of the barrier model during the standing-up operation and the behaviour of the barrier at the wave-overtopping operation after standing-up were conducted through structural analysis that it exerts excellent performance. However, there remains a need to consider that a proper design method for supporting the hinge and the roller frame in the future.

#### Acknowledgement

The research was a part of the project titled 'Development of Movable Barrier on shore for Disaster Mitigation by Storm Surge and Abnormal high wave (2018)', funded by the Ministry of Oceans and Fisheries (MOF), Korea (project No. 20170039)

#### References

- Coastal Development Institute of Technology, 2001. Research and development of numerical wave channel. CDIT Library, 12 (in Japanese).
- Coastal Development Institute of Technology, 2010. Research and development of numerical wave tank (CAD-MAS-SURF/3D). CDIT Library, 39 (in Japanese).
- Engelund, F.A., 1953. On the laminar and turbulent flows of ground water through homogeneous sand. Danish Academy of Technical Sciences.
- Hirt, C.W. & Nichols, B.D., 1981. Volume of fluid (VOF) method for the dynamics of free boundaries. *Journal of Computational Physics*, 39(1), 201-225.
- Hoyle, B.S., 1989. The port—City interface: Trends, problems and examples, *Geoforum*, 20(4) p. 429-435.
- MLTM (Ministry of Land, Transport and Maritime Affairs), 2011. A case study on the redevelopment of disaster vulnerability districts in harbour by climate change (Aramir project), Korea (in Korean).
- Sakakiyama, T., Abe, N. & Kajima, R., 1990. Analysis of nonlinear wave around permeable structure by porous model. *Proceedings of Coastal Engineering, JSCE*, 37, 554-558 (in Japanese).
- Simulia (2013) ABAQUS
- Sha, W.T., Domanus, H.M., Schmitt, R.C., Oras, J.J. & Lin, E.I.H., 1978. *COMMIX-1: A three dimensional transient single-phase component computer program for thermal-hydraulic analysis*. Argonne National Laboratory, NUREG/CR-0785, ANL-77-96.